Fish and Shellfish Immunology 88 (2019) 272–283

Contents lists available at ScienceDirect

Fish and Shellfish Immunology

journal homepage: www.elsevier.com/locate/fsi

Full length article

Transcriptome analysis of the spleen provides insight into the immunoregulation of *Mastacembelus armatus* under *Aeromonas veronii* infection

Chong Han[a,1], Qiang Li[b,1], Qinghua Chen[c], Guofeng Zhou[a], Jianrong Huang[a,*], Yong Zhang[a,**]

[a] State Key Laboratory of Biocontrol, Institute of Aquatic Economic Animals and Guangdong Provincial Key Laboratory for Aquatic Economic Animals, School of Life Sciences, Sun Yat-Sen University, Guangzhou, PR China
[b] School of Life Sciences, Guangzhou University, Guangzhou, PR China
[c] South China Institute of Environmental Science, MEP, Guangzhou, PR China

ARTICLE INFO

Keywords:
Mastacembelus armatus
Aeromonas veronii
Transcriptome
Differentially expressed gene
Immune

ABSTRACT

Mastacembelus armatus, also known as the zigzag eel, is an economically important species of freshwater fish that is very popular with consumers as a high-grade table fish in China. Recently, the wild population of this fish has declined gradually due to overfishing and various types of ecological imbalance. Meanwhile, the aquaculture of this spiny eel has flourished in southern China. To understand the immune response of zigzag eel to *Aeromonas veronii*, we carried out transcriptome sequencing of zigzag eel spleens after artificial bacterial infection. After assembly, 110,328 unigenes were obtained with 44.42% GC content. A total of 27,098 unigenes were successfully annotated by four public protein databases, namely, Nr, UniProt, KEGG and KOG. Differential expression analysis revealed the existence of 1278 significantly differentially expressed unigenes at 24 h post infection, with 767 unigenes upregulated and 511 unigenes downregulated. After GO and KEGG enrichment analyses, many immune-related GO categories and pathways were significantly enriched. The typical significantly enriched pathways included toll-like receptor signaling pathway, cytokine-cytokine receptor interaction and TNF signaling pathway. In addition, 40,027 microsatellites (SSRs) and 52,716 candidate single nucleotide polymorphisms (SNPs) were identified from the infection and control transcriptome libraries. Overall, this transcriptomic analysis provided valuable information for studying the immune response of zigzag eels against bacterial infection.

1. Introduction

Mastacembelus armatus, also known as the zigzag eel, is an economically important inland water species belonging to the Mastacembelidae family in the Synbranchiformes order [1]. The species usually inhabits in streams and rivers with sand, pebble or boulder substrates [2]. *M. armatus* is mainly distributed in southern China including Yunnan, Guizhou, Guangxi, Guangdong, Fujian and Hainan provinces. Due to the good flavor and high nutritional value of *M. armatus*, this species is very popular with consumers as a high grade table fish [2,3]. Meanwhile, *M. armatus* is also popular as an aquarium fish in Asian countries owing to its beautiful skin texture [3]. However, the wild population of *M. armatus* has declined gradually in recent years due to overfishing and environmental disruption. According to the ministry of agriculture of the People's Republic of China, three national aquatic germplasm resource reserves of zigzag eels have been established to intensify conservation efforts. Recently, consumer demand for high-quality aquatic products is growing fast, and the scale of zigzag eel

Abbreviations: SSR, Microsatellite; SNP, Single nucleotide polymorphism; LB, Luria-Bertani; PBS, Phosphate buffered saline; GO, Gene ontology; KOG, EuKaryotic Orthologous Group; KEGG, Kyoto Encyclopedia of Genes and Genomes; FDR, False discovery rate; TPM, Transcripts per million; qRT-PCR, Quantitative real-time PCR; TLR, Toll-like receptors; IL, Interleukin; TNF, Tumour necrosis factors; NF-κB, Nuclear factor kappa-B; NFKBIA, NF-kappa-B inhibitor alpha; IKKE, Inhibitor of nuclear factor kappa-B kinase; CSF, Colony stimulating factor; TGF, Transforming growth factor

* Corresponding author. State Key Laboratory of Biocontrol, Institute of Aquatic Economic Animals and Guangdong Provincial Key Laboratory for Aquatic Economic Animals, School of life Sciences, Sun Yat-Sen University, 135 Xingang Road West, Guangzhou, 510275, PR China.
** Corresponding author.
E-mail addresses: lsshjr@mail.sysu.edu.cn (J. Huang), lsszy@mail.sysu.edu.cn (Y. Zhang).
[1] These authors contributed equally to this work.

https://doi.org/10.1016/j.fsi.2019.02.020
Received 8 May 2018; Received in revised form 7 February 2019; Accepted 13 February 2019
Available online 14 February 2019

aquaculture has increased rapidly.

Aeromonas veronii is a gram-negative pathogen that comprises motile stains and grows well at 35–37 °C [4]. This species has been characterized as a "highly virulent pathogen" that can cause motile aeromonad septicemia in both fish and mammals [5]. Together with *Aeromonas hydrophila*, *A. veronii* has had devastating effects on the fishing industries of various fish species and has led to disastrous economic losses for farmers [6,7]. *A. veronii* has been reported to cause motile aeromonad septicemia in many cultured fish species including common carp [8], Nile tilapia [9] and rainbow trout [10]. Zhang et al. [11] isolated 143 bacterial strains from 15 species of diseased fishes in southern China and found that approximately 56% of the bacterial strains were *A. veronii* and 28% were *A. hydrophila*, indicating that *A. veronii* was the primary *Aeromonas* species infecting freshwater fish in southern China.

Understanding the immune defense mechanism of zigzag eels against *A. veronii* is very important for the control and prevention of bacterial infection. However, previous studies have mainly focused on the biology [12–14], histophysiology [15–17] and population genetics [18] of this species, with only a few studies mentioning immune analysis [19,20]. Uthayakumar et al. [19] performed a biochemical characterization of the skin mucus of zigzag eels and concluded that the mucus extracts exhibited higher inhibitory activity than the antibiotic ampicillin against bacterial and fungal pathogens. Han et al. [20] suggested that the expression of TLR3 and TLR5M would change substantially after infection with *Vibrio parahaemolyticus*. To date, no study has been performed on the response of *M. armatus* to *A. veronii* stimulation.

In recent years, next-generation sequencing technologies have developed rapidly and transcriptome sequencing technologies have been widely used for genomic research, identification of functional genes and gene expression analysis especially in non-model organisms. Comparative transcriptomic analysis has emerged as a cost-effective analytical strategy to study immune response against pathogens in teleost fish [21–23]. For instance, 2900 significantly differentially expressed genes were identified by comparing an experimental group infected with *A. hydrophila* and a control group of common carp [21]. After infection with *A. hydrophila*, 1104 unigenes were significantly upregulated and 1304 unigenes were downregulated in golden mahseer liver, and these genes were mainly involved in immune-related pathways [22]. Tran et al. [23] analyzed the transcriptome sequencing results of blunt snout bream before and after infection with *A. hydrophila* and identified 53 significantly differentially expressed unigenes related to the immune system. To date, there have been no published omics analyses of zigzag eels.

In this study, we used an Illumina HiSeq 4000 system to analyze the transcriptomic profiles of zigzag eels after infection with *A. veronii*. After assembly and annotation, many functional genes were identified. In addition, many significantly differentially expressed genes were identified and were seen to be mainly enriched in immune related GO categories and pathways. Moreover, a great number of microsatellite (SSR) and single nucleotide polymorphism (SNP) markers were developed, which will be useful in population genetic analysis and selective resistance breeding. Overall, this study is the first comparative transcriptomic analysis of zigzag eels and systematically describes the immune response against *A. veronii* infection. The results of this study will provide valuable information for future genetic and genomic research on zigzag eels.

2. Materials and methods

2.1. Fish, bacterial challenge and sampling

Healthy *M. armatus* samples with an average body weight of 30±10 g were purchased from the Zengcheng aquatic products market in Guangzhou city and maintained in the laboratory at room temperature. During the whole experimental period, all the zigzag eels were fed bloodworms twice a day (9:00 a.m. and 6:00 p.m.), and two-thirds of the water in tanks was changed every day. The *A. veronii* bacterial strains were obtained from Guangdong Microbial Culture Collection Center. After scaling up the cultivation using LB broth, the bacterial concentration was determined by plate-based colony-counting methods. Approximately 5 mL 10^{10} and 10^{8} CFU/mL bacterial suspensions diluted in PBS were separately prepared for subsequent challenge.

After acclimatization for ten days, 40 healthy zigzag eel specimens were randomly divided into a control group and an infection group. Before the actual experiment, we performed three pre-experiments by injecting the fish intraperitoneally with 200 μL of the 10^{10} CFU/mL bacterial suspension to confirm that *A. veronii* injection made healthy zigzag eel weak or caused death. During the actual experiment, each fish in the infection group was injected intraperitoneally using 100 μL of 1.0×10^{8} CFU/mL bacterial suspension, and each fish in the control group was injected in an identical manner with 100 μL of PBS. At 24 h post-injection, nine fish from each group were randomly divided into three replicates (three fish per replicate) and then anesthetized using MS-222 (Sigma, USA). The spleen tissues of the fish were immediately collected and immersed in RNA Keeper Tissue Stabilizer (Vazyme, China), kept overnight at 4 °C, and then moved to −20 °C until RNA extraction.

2.2. Detection of the effect of injection

In our pre-experiment, the three zigzag eels injected intraperitoneally with 200 μL of 10^{10} CFU/mL bacterial suspension all died by 24 h post-injection, suggesting that *A. veronii* injection caused death of healthy zigzag eels. In the actual experiment, the zigzag eels in the infection and control groups all appeared to behave normally until 48 h post injection with the death of only two specimens observed in the experimental group by 24 h post-injection.

In addition, we tested the tissue distribution of *A. veronii* in two zigzag eels from each group using specific primers designed according to the 16S rDNA sequence of *A. veronii* (F: 5′-TGCCAGCTGTGACGTTA CTC-3′, R: 5′-TACTTCTGGTGCAACCCACT-3′). The test results showed that *A. veronii* was present in the livers, gills, intestines, spleens and kidneys of infected fish, while no *A. veronii* was detected in any of the examined tissues of control fish (Fig. 1). Furthermore, we selected some

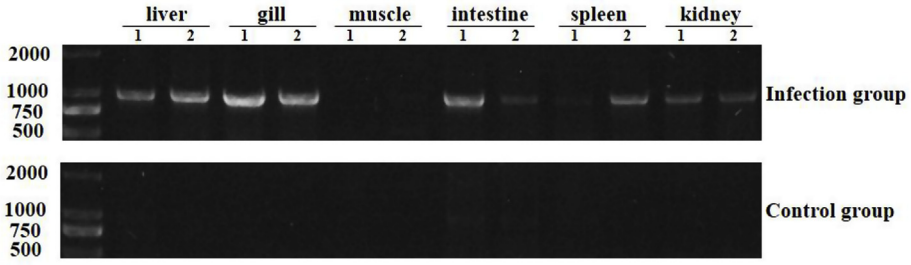

Fig. 1. Electrophoretic analysis of *A. veronii* in different tissues of *M. armatus* in the control and infection groups.

PCR products with bands corresponding to the target gene to perform DNA sequencing. As expected, BLAST analysis revealed that all the obtained sequences matched with the 16S rDNA sequence of *A. veronii*.

2.3. RNA extraction, cDNA library construction and illumina sequencing

The total RNAs from the spleen of each fish was extracted according to the manufacturer's instructions for the RNA Isolater Total RNA Extraction Reagent (Vazyme, Nanjing). The integrity and quality of the total RNA were monitored using an Agilent 2100 bioanalyzer. As mentioned above, equal quantities of RNA from each fish from one replicate were pooled and triplicate of RNA samples from the experimental and control groups were generated and used for cDNA library construction.

Sequencing libraries were constructed using the NEBNext® Ultra™ RNA Library Prep Kit for Illumina® (NEB, USA) following the manufacturer's instructions. First, total RNA was purified using oligo(dT) attached magnetic beads to enrich poly(A) mRNA. Second, the obtained mRNAs were fragmented into small pieces using the NEBNext FirstStrand Synthesis Reaction Buffer (5×). Then, first-strand cDNA was synthesized using M-MLV Reverse Transcriptase and a random hexamer primer, and the second cDNA strand was synthesized using DNA polymerase I and RNase H. Subsequently, the synthesized double-stranded cDNAs were purified using the QIAquick PCR Purification Kit (Qiagen, Germany), subjected to end-repair, and addition of poly (A), ligated to the sequencing adaptors. PCR amplification was performed to enrich the purified cDNA. Finally, the cDNA libraries were sequenced using an Illumina HiSeq 4000 system.

2.4. Assembly and annotation

Raw reads were trimmed to generate clean reads after removing the adaptor sequences, repeated reads and low-quality reads. The obtained clean reads were assembled using Trinity software with default parameters [24] for de novo transcriptome assembly. Then, the reads were mapped back to the contigs. The contigs from the same transcript and the distances between the contigs could be detected based on paired-end reads. Subsequently, scaffolds were further generated by connecting the contigs with the unknown sequences between contigs represented by N. Finally, the gaps between the scaffolds were filled to generated unigenes.

All obtained unigenes were searched against the NCBI Nr, UniProt, KOG and KEGG public databases using BLAST similarity search with an E-value threshold of 1.0E-5. Based on the Nr annotation, Blast2GO software was used to obtain GO annotations of the unigenes [25]. Furthermore, the WEGO web tool (http://wego.genomics.org.cn/cgibin/wego/index.pl) was used to obtain GO functional classification at the macro level [26]. In addition, the KOG database was also used to predict and identify the functional categories of the unigenes (https://www.ncbi.nlm.nih.gov/Structure/cdd/wrpsb.cgi). Finally, KEGG pathway mapping was performed to determine pathway assignments [27].

2.5. Identification of differentially expressed genes and enrichment analysis

The expression levels of the unigenes were determined by mapping the clean reads from different libraries back to the transcriptome assembly using Bowtie 2 software [28]. The TPM (transcripts per million) method was used to calculate the expression levels of the unigenes from different replicates. The false discovery rate (FDR) was calculated and used to determine the threshold of the P-values. The significantly differentially expressed genes between the experimental and control groups were determined with an FDR ≤ 0.05 and an absolute value of $\log_2$ratio ≥ 1. Heat map analysis was performed using OmicShare, a free online platform for data analysis (http://www.omicshare.com/tools).

GO classification and KEGG analysis of the differentially expressed unigenes were performed to further understand the detailed functional attributes of the genes using the hypergeometric distribution test. The obtained GO categories with $p < 0.05$ and pathways with q-value ≤ 0.05 were defined as significantly enriched GO classifications and KEGG pathways.

2.6. Quantitative real-time PCR

To validate the reliability of our transcriptome sequencing data, a total of 14 differentially expressed immune related genes were selected randomly for quantitative real-time PCR (qRT-PCR) analysis. Specific primers were designed using Primer Premier 5.0 based on the sequences of 14 differentially expressed immune-related genes and β-actin (Table S1). The template cDNAs used for qRT-PCR analysis were the same as those used for library construction. Each qRT-PCR amplification was carried out using AceQ qPCR SYBR Green Master Mix (Vazyme, Nanjing) on a LightCycle 480 system according to manufacturer's instructions. The qRT-PCR profiles included an initial denaturation step at 95 °C for 2 min, followed by 40 cycles of 95 °C for 10 s, 60 °C for 20 s and 72 °C for 20 s. Dissociation curve analysis was performed following each PCR reaction to confirm only one target product was amplified. All reactions were performed in triplicate wells. The obtained results were normalized using β-actin and the comparative CT method ($2^{-\triangle\triangle CT}$) [29]. In addition, several TLRs identified from our transcriptome data were also selected to analyze the expression pattern after bacterial infection at different time points (12, 24 and 48 h).

2.7. SSR detection and SNP calling

In our transcriptome sequencing data, all the potential SSR motifs were searched against all the unigenes using MISA (http://pgrc.ipk-gatersleben.de/misa/) [30]. The mono-to hexanucleotide repeats with at least four repeat units were all considered to be SSR motifs. Primers were also designed for most SSRs using Primer 3 [31]. Putative single nucleotide polymorphisms (SNPs) were detected using SOAPsnp software by mapping against all reference unigenes [32]. The transition and transversion counts were also calculated.

3. Results

3.1. Transcriptome sequencing and assembly

Three duplicate spleen samples of spleen from both the control group (MC) and the *A. veronii*-infected experimental group (MA) were sequenced at 24 h post injection using Illumina-based transcriptome sequencing. After quality control and data filtering, each sequencing library generated more than 24 million clean reads, with Q30 greater than 90% (Table 1). Raw sequencing reads were submitted to the NCBI transcriptome shotgun assembly (TSA) database under the accession numbers: SRR7125338, SRR7125339, SRR7125340, SRR7125341, SRR7125342, and SRR7125343.

A total of 110,328 unigenes were generated via transcriptome

Table 1
Summary of transcriptome sequencing results.

Samples	Read length (bp)	Number of bases (bp)	Number of clean reads	Q30 (%)	Number of detected gene
MC1	150	8,905,755,900	29,685,853	93.53	62,955
MC2	150	7,398,657,600	24,662,192	91.78	58,063
MC3	150	7,645,004,400	25,483,348	91.51	56,752
MA1	150	7,390,300,800	24,634,336	91.70	56,411
MA2	150	8,509,326,000	28,364,420	90.63	56,293
MA3	150	8,432,755,500	28,109,185	91.545	54,643

Table 2
Summary of assembled unigenes obtained from transcriptome analysis.

Description	Number
Unigenes	110,328
Total length (bp)	106,589,793
Average length (bp)	966
N50	2420
Max length (bp)	25,983
Min length (bp)	201
GC (%)	44.42

assembly, with an N50 length of 2420 bp. The minimum and maximum lengths of the unigenes were 201 and 25,983 bp, respectively, and the GC content was 44.42% (Table 2). The length distribution of the unigenes showed that 52,995 unigenes (48.03%) had lengths ranging from 301 to 1000 bp (Fig. S1).

3.2. Annotation of all unigenes

Out of 110,328 unigenes, 27,098 (24.56%) were successfully annotated using the BLASTx algorithm against Nr, UniProt, KEGG and KOG databases, while 83,230 (75.44%) were not annotated. Among these unigenes, 26,669 (24.17%) were annotated by UniProt and 26,215 (23.76%) were in the Nr database. In addition, 11,710 (10.61%) unigenes were annotated by all four public protein databases (Fig. S2). Moreover, the E-values, identities and scores of the unigenes assigned by the Nr database were calculated. The E-value distribution showed that approximately 73% of the annotated unigenes were significantly homologous to the deposited sequences (with E-values less than 1.0E-50), with the remaining 27% exhibiting E-values ranging from 1.0E-50 to 1.0E-10 (Fig. 2A). The score distribution showed that 4576 (17%) unigenes had scores greater than 1000, and 18,848 (72%) had scores between 100 and 1000 (Fig. 2B). The identity distribution demonstrated that approximately 75% of the annotated unigenes exhibited identities greater than 75%, with only 4% exhibiting identities less than 50% (Fig. 2C). In addition, the distribution of BLASTx top-hit species showed that 14,001 unigenes (51.67%) matched with sequences from *Lates calcarifer*, which had the highest match ratio (Fig. 2D).

For functional classification, all the assembled unigenes were further assigned to GO, KOG and KEGG categories. In the GO classification, 20,780 unigenes were categorized into 47 GO terms belonging to three domains: biological process, cellular component and molecular function. The detailed annotation revealed that the top clustered class was binding (10,632, 51.16%), which was followed by cellular process (9768, 47.01%), metabolic process (7525, 36.21%), catalytic activity (7246, 34.87%) and membrane part (7035, 33.85%). In addition, 816 (3.93%) and 240 (1.15%) unigenes were assigned to response to stimulus and immune system process, respectively (Table S2).

A total of 15,219 unigenes were aligned to 25 functional categories in the KOG database. As shown in Fig. 3, the largest category was General function prediction only, containing 2656 unigenes (17.45%), which was followed by Signal transduction mechanisms (2227,

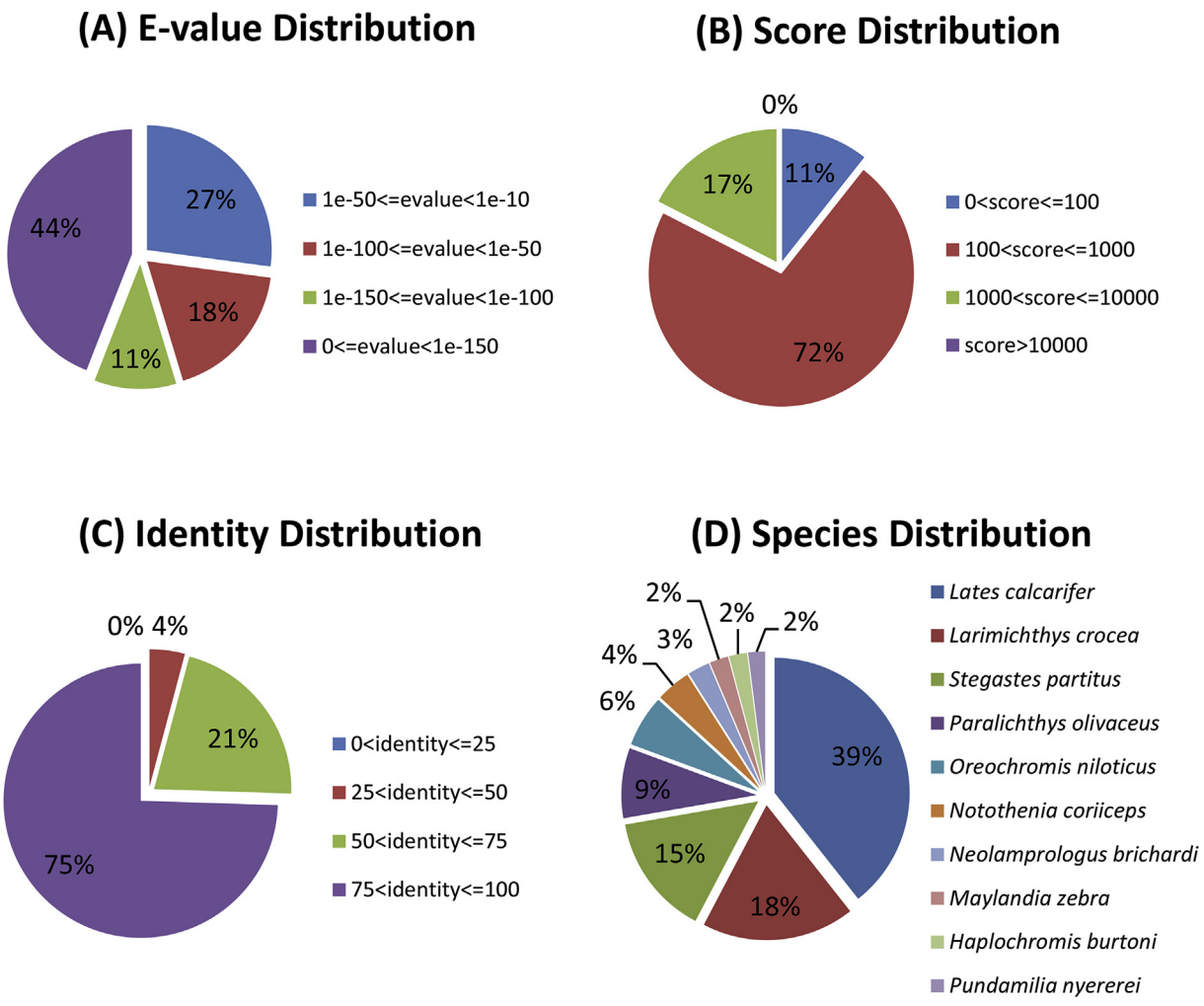

Fig. 2. E-value (A), score (B), identity (C) and species (D) distribution based on the Nr database.

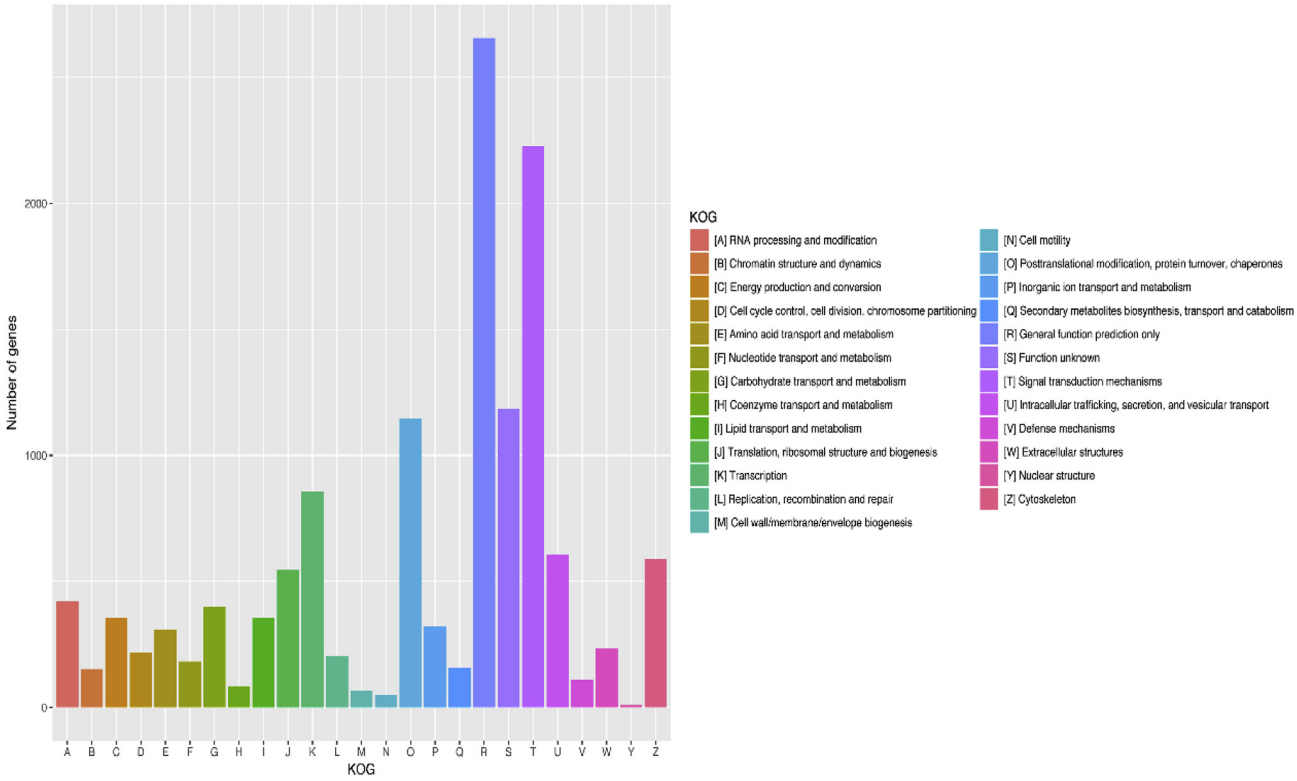

Fig. 3. Histogram presentation of EuKaryotic Orthologous Groups (KOGs).

14.63%), Function unknown (1186, 7.79%) and Posttranslational modification, protein turnover, chaperones (1147, 7.54%). Only 9 unigenes were assigned to Nuclear structure.

The KEGG database was used to classify the biological pathways of unigenes. A total of 16,523 unigenes were annotated by this database and further categorized into 46 level-2 KEGG pathways and 387 level-3 KEGG pathways. Among the 46 level-2 KEGG pathways, Signal transduction was the predominant category containing 2818 unigenes, which was followed by Global and overview maps (1635, 9.9%), Cancers: Overview (1608, 9.73%) and Immune system (1370, 8.29%) (Table S3). The predominant level-3 KEGG pathway was Metabolic pathways (1574, 9.53%), which was followed by Pathways in cancer (831, 5.03%) (Table S4).

3.3. Differential expression analysis

In this study, a total of 1278 unigenes (1882 contigs) with FDR ≤ 0.05 and absolute value of $\log_2$ratio ≥1 were identified as differentially expressed genes. Among these genes, 757 unigenes (1248 contigs) were upregulated in the infection group while 511 unigenes (636 contigs) were downregulated (Table S5). In addition, a heatmap was generated to visualize the expression levels of the differentially expressed genes in six transcriptome sequencing samples (Fig. 4). The cluster analysis showed that there was a large difference in overall expression pattern between the MA and MC groups. After infection, most genes were upregulated with a handful of genes exhibiting downregulation in three duplicates of experimental group.

To further understand the detailed functional classification of these differentially expressed genes, GO and KEGG enrichment analyses were performed for these genes. According to the GO analysis, 1148 unigenes were grouped into 43 GO terms (Fig. 5). The top five clustered classes were binding (563), cellular process (485), membrane part (435), catalytic activity (404) and metabolic process (379). Out of the 43 GO terms, six terms were significantly enriched ($p < 0.05$) primarily extracellular region part (38), immune system process (30), response to stimulus (67), multi-organism process (10) and locomotion (19) (Table S6).

In the KEGG annotation, a total of 838 unigenes were included in 44 level-2 KEGG pathways. As shown in Fig. 6, Signal transduction was the largest category containing 167 unigenes, which was followed by Cancers: Overview (107), Immune system (106) and Infectious diseases: Viral (88). Moreover, the differentially expressed genes were also assigned to 328 level-3 KEGG pathways. Metabolic pathways was the predominant category (82); however many immune-related pathways also exhibited unigene enrichment, including Pathways in cancer (57), HTLV-I infection (36), Cytokine-cytokine receptor interaction (35), Human papillomavirus infection (33). Moreover, many differentially expressed genes were also enriched in other important immune-regulation pathways, such as the NOD-like receptor signaling pathway, MAPK signaling pathway, Jak-STAT signaling pathway and NF-kappa B signaling pathway (Table S7). In addition, the results of the significance test for these pathways revealed that 16 pathways were significantly enriched (Q-value ≤ 0.05), and all of these pathways including toll-like receptor signaling pathway, cytokine-cytokine receptor interaction and TNF signaling pathway, participated in immune regulation (Table 3). In addition, some pathways associated with viral disease (HTLV-I infection) and parasitic disease (Leishmaniasis, Malaria, Chagas disease) were also significantly enriched (see Table 3).

3.4. qRT-PCR

In this study, we detected 14 immune-related differentially expressed genes using qRT-PCR analysis to validate the Illumina sequencing data. The melting-curve analysis showed that only one product was amplified in each PCR. Fold changes deduced from qRT-PCR and Illumina analyses were compared. As shown in Fig. 7, all the tested genes showed similar trends in up- or down-regulation in the results of the qRT-PCR and transcriptome sequencing analyses, which indicated that the transcriptome sequencing data reflected actual gene expression profiles in *M. armatus* infected with *A. veronii*. Considering that the

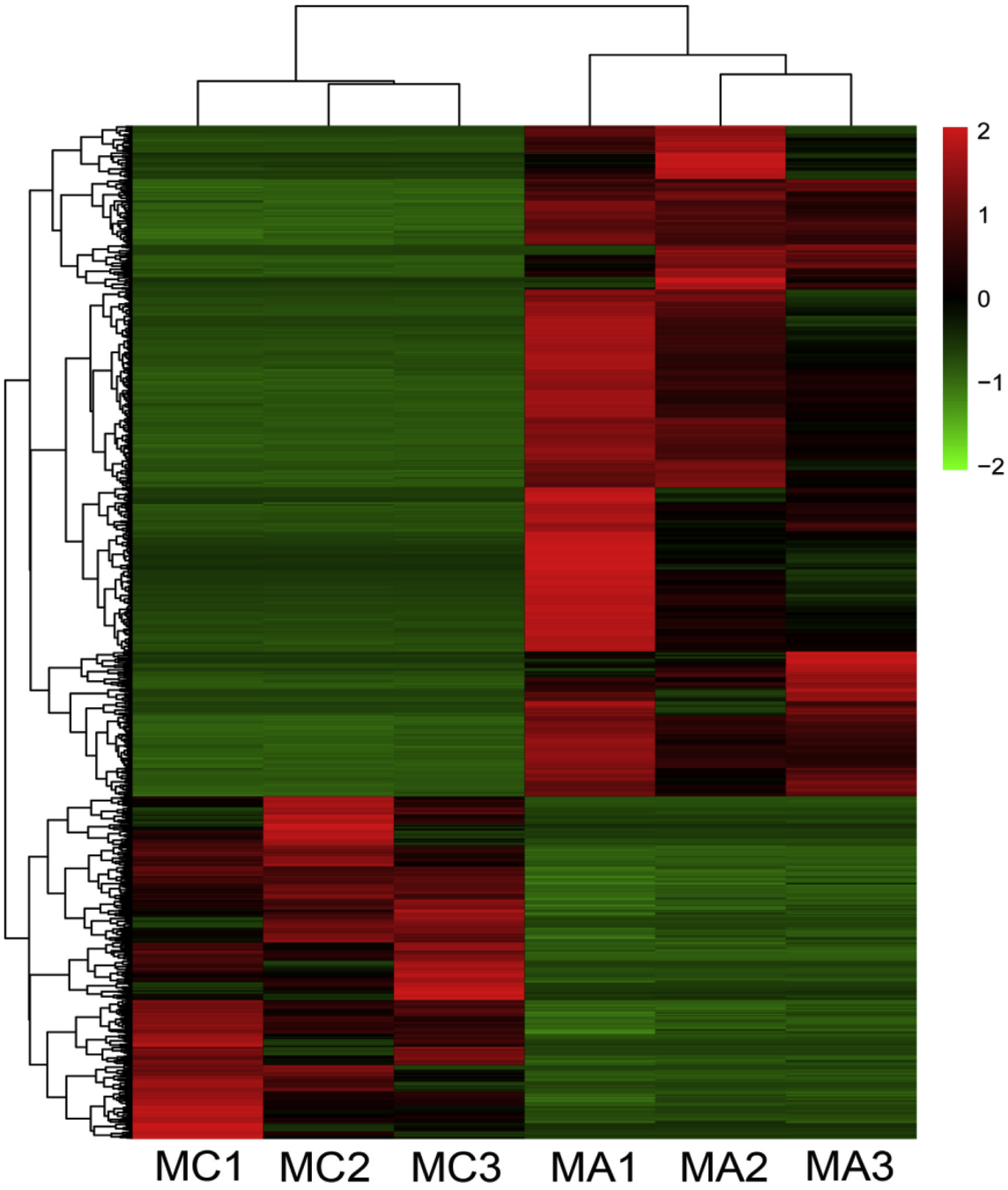

Fig. 4. Heatmap analysis of differentially expressed genes in each sequencing library. Each column represents a sequencing sample and each row represents a gene. The red region indicates upregulation and the green region indicates down-regulation. (For interpretation of the references to colour in this figure legend, the reader is referred to the Web version of this article.)

expression levels of TLRs may rely on the length of infection period, we further analyzed the expression levels of several TLRs at three different time points after bacterial infection. Among nine TLRs, only TLR5S were significantly upregulated at 12 and 24 h post infection, while TLR5M was increased a little at 24 h. Furthermore, TLR2, TLR7, TLR14, TLR21 and TLR23 were all significantly downregulated at 12 h post infection, and then increased gradually at following time points. Only the expression level of TLR22 did not change significantly at all time points (Fig. 8).

3.5. Identification of SSRs and SNPs

All the assembled unigenes were used to mine for potential SSR markers (see Table 4). A total of 40,027 SSRs were identified from 27,694 unigenes, and 7672 unigenes contained more than one SSR. Among these SSRs, mononucleotide repeats were the most abundant type with 24,608 mononucleotide repeats observed, which was followed by di-nucleotide (10,027), tri-nucleotide (3130), tetra-nucleotide (1743), penta-nucleotide (422) and hexa-nucleotide repeats (97) (Table 2). The SSRs with mononucleotide repeats all contained more than ten repeat units and 3802 loci contained 6 repeat units (Table S8). In addition to mononucleotide repeats, the dominant SSR motifs were AC/GT (7196) and AG/CT (1480) (Table S9). We also further designed primers for SSRs with di-to tetra-nucleotide repeats (Table S10).

Furthermore, a total of 52,716 candidate SNPs including 33,672 transitions and 19,044 transversions, were identified from the infection

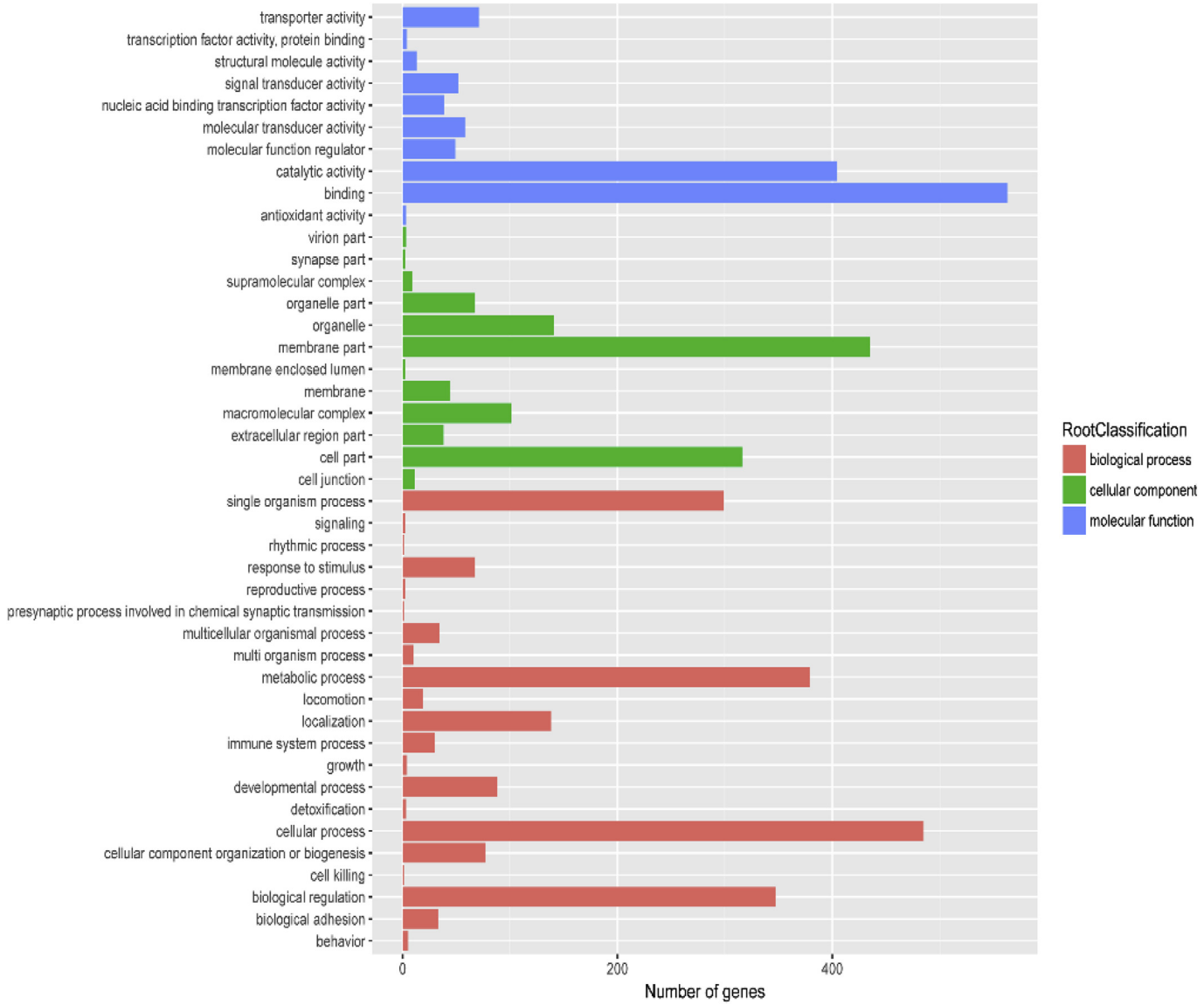

Fig. 5. Scatter chart of Gene Ontology classification of differentially expressed genes.

and control transcriptome libraries. As shown in Fig. 9, the different transition types (A/G, C/T) and transversion types (A/T, A/C, G/T, C/G) exhibited good agreement, respectively. All the potential SNP markers require experimental testing to eliminate false positives and sequencing errors.

4. Discussion

M. armatus is an economically important freshwater fish in south China. The wild population of this fish has decreased by the day in recent years, and aquaculture of zigzag eels has developed rapidly. However, no study has been performed to elucidate the molecular mechanism of disease defense in zigzag eels. Recently, de novo transcriptome sequencing has been widely used in teleost fish due to the low cost and high throughput of this method [21–23]. Comparative transcriptomic analysis has been widely used as a robust strategy to understand the physiological response to various stimuli [33]. In this study, for the first time, comparative transcriptomic analysis was performed to assess the transcriptional response in the spleens of zigzag eels after infection with *A. veronii*. In addition, many differentially expressed genes were found to participate in immune regulation against pathogen infection.

A total of 110,328 unigenes were obtained in our transcriptome assembly, with an average length of 966 bp, which is longer than that reported in spotted halibut (938 bp) [34] and blunt snout bream (692 bp) [23]. However, out of the 110,328 unigenes, 86,391 (78.3%) unigenes could not be identified by four public protein databases, and might represent novel transcripts or invalid sequences due to assembly error [35,36]. According to GO classification, binding, cellular process and metabolic process were the predominant categories, as seen in other fish species, such as miiuy croaker [37] and spotted halibut [34]. Similar to spotted halibut [34], Signal transduction was the most enriched category in the KEGG pathway analysis. A total of 1278 (1.16%) significantly differentially expressed unigenes were identified, which is much less than the number reported for darkbarbel catfish spleen after infection with *A. hydrophila* (27,803, 7.21%) [38]. Among the KEGG pathways, 16 immune-related pathways were significantly enriched, including some inflammatory response pathways such as toll-like receptor signaling pathway, cytokine-cytokine receptor interaction and TNF signaling pathway, which suggested that the injection of *A. veronii* induced a strong inflammatory response in *M. armatus* spleen.

Toll-like receptors (TLRs) are important pattern-recognition receptors that play an important role in the recognition of pathogen-associated molecular patterns including lipopolysaccharides,

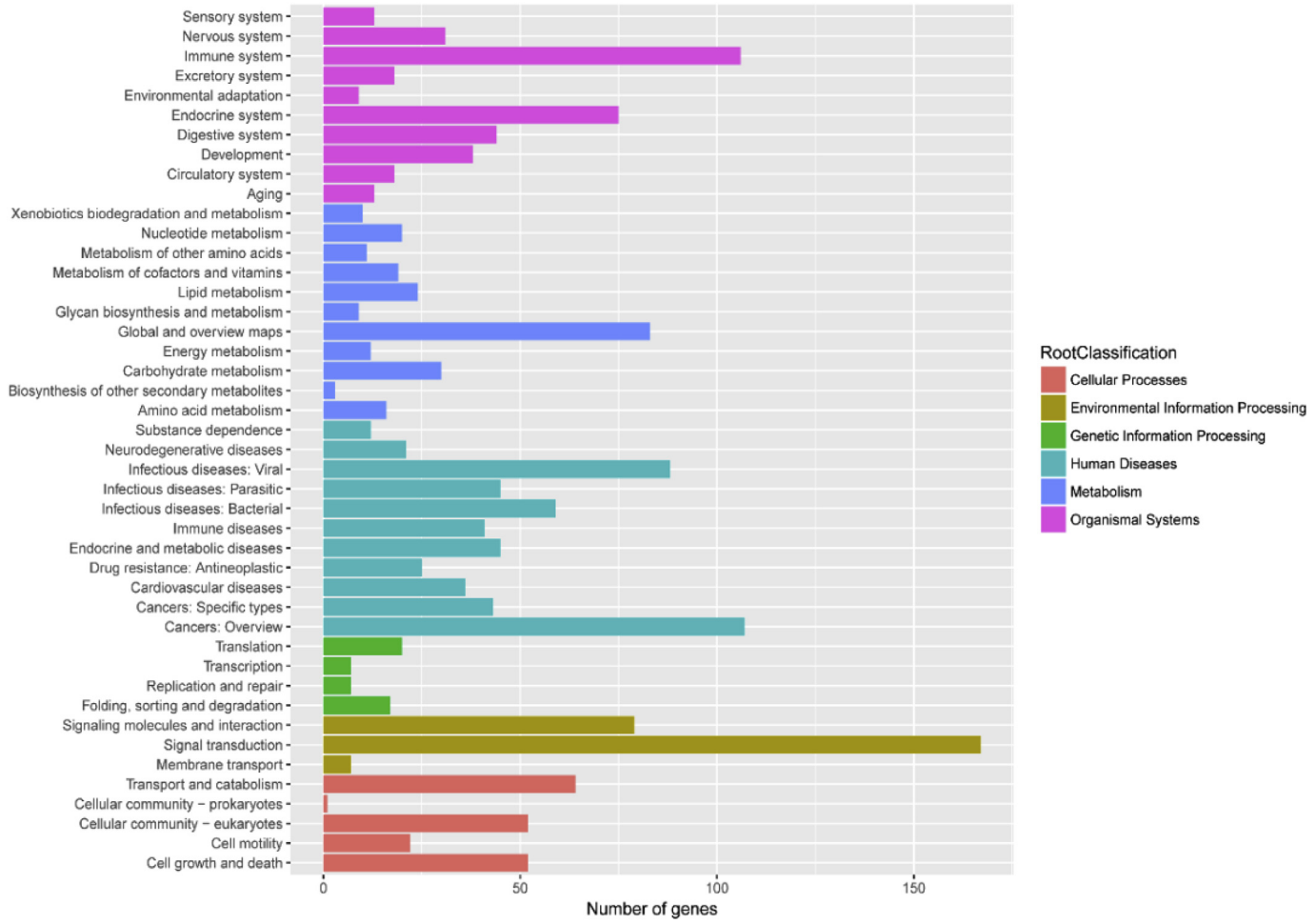

Fig. 6. Scatter chart of KEGG pathway enrichment of differentially expressed genes.

Table 3
Significantly enriched KEGG pathways of differentially expressed genes.

KEGG Pathway	No. of differentially expressed genes	All unigenes annotated in pathway	Ratio	Q-value
Cytokine-cytokine receptor interaction	35	224	15.63%	1.17E-06
Rheumatoid arthritis	20	97	20.62%	1.21E-05
Hematopoietic cell lineage	19	97	19.59%	3.88E-05
Inflammatory bowel disease (IBD)	16	75	21.33%	6.91E-05
Leishmaniasis	16	90	17.78%	6.65E-04
Toll-like receptor signaling pathway	18	117	15.38%	1.29E-03
Malaria	12	59	20.34%	1.37E-03
Chagas disease	20	159	12.58%	5.55E-03
Allograft rejection	10	50	20.00%	5.55E-03
Antifolate resistance	9	42	21.43%	5.55E-03
Type I diabetes mellitus	11	63	17.46%	7.36E-03
Measles	17	132	12.88%	9.44E-03
HTLV-I infection	36	401	8.98%	1.90E-02
Graft-versus-host disease	8	44	18.18%	2.68E-02
TNF signaling pathway	17	154	11.04%	4.16E-02
Pertussis	13	105	12.38%	4.33E-02

lipopeptides, flagellins, and dsRNAs [39,40]. The TLR gene family can be activated by infection with *Aeromonas*, as has been widely reported in teleost fish such as common carp and blunt snout bream [41,42]. In this study, the TLR signaling pathway was significantly enriched, according to the KEGG enrichment analysis of the differentially expressed genes. In humans, TLR5 can trigger the MyD88-dependent signaling pathway and activate the transcription factor Nuclear factor kappa B (NF-κB), inducing the transcription of proinflammatory cytokines such as interleukin-1 (IL-1) and tumour necrosis factor alpha (TNF-α) after flagellin recognition [43]. In our study, TLR5M, TLR5S and downstream proinflammatory cytokines, including IL1β, IL8, IL12 and TNF 2, were significantly upregulated in the spleens of zigzag eels after infection with *A. veronii* (Fig. S3), which suggested that TLR5M and TLR5S participate in the recognition of *A. veronii* and activate the MyD88-dependent signaling pathway in the spleens of zigzag eels. Besides, according to the transcriptome and qPCR results, the expression of TLR5S was higher than TLR5M at 24 h post infection. The qPCR results at three different time points also showed that TLR5S had

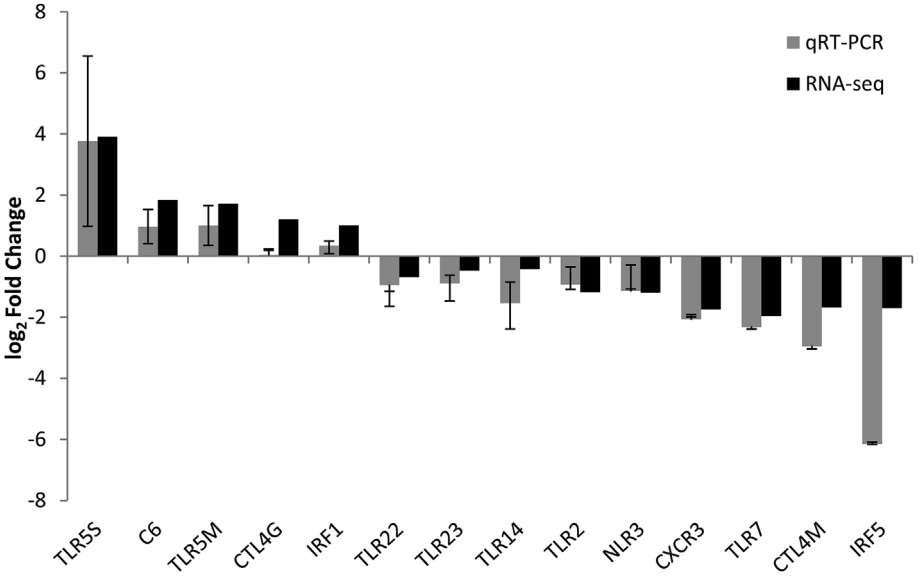

Fig. 7. Comparison of the expressions of transcriptome sequencing and qRT-PCR results.

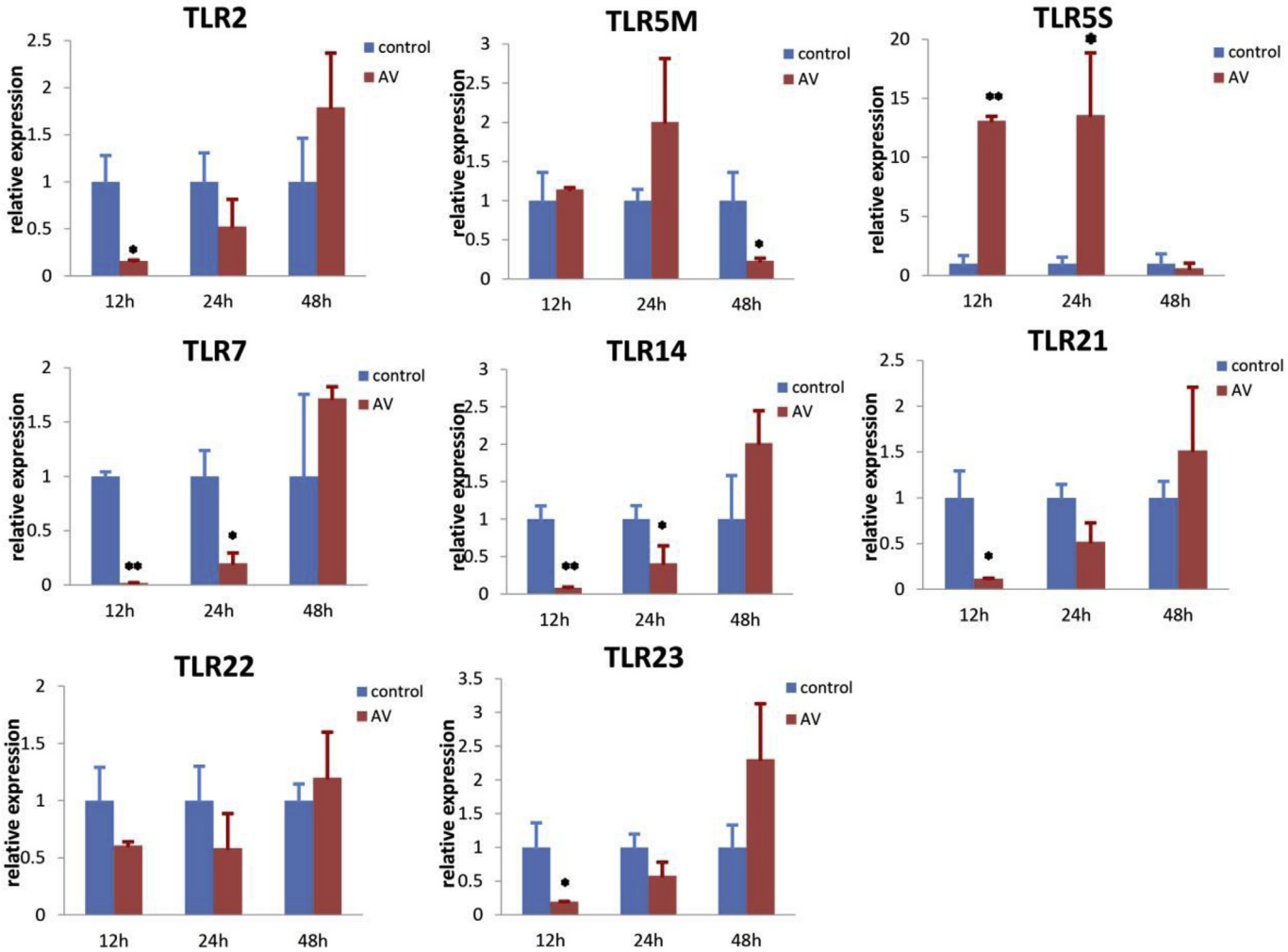

Fig. 8. The mRNA expression levels of TLR2, TLR5M, TLR5S, TLR7, TLR14, TLR21, TLR22 and TLR23 were analyzed by qPCR. All the results were evaluated by normalizing to the reference genes (β-actin). Mean ± SD (n = 3), $*P < 0.05$, $**P < 0.01$.

Table 4
Summary of SSR identification.

Description	Number
Total number of sequences examined	110,328
Total size of examined sequences (bp):	106,589,793
Total number of identified SSRs:	40,027
Number of SSR-containing sequences:	27,694
Number of sequences containing more than 1 SSR:	7672
Mononucleotide	24,608
Di-nucleotide	10,027
Tri-nucleotide	3130
Tetra-nucleotide	1743
Penta-nucleotide	422
Hexa-nucleotide	97

already been significantly upregulated at 12 h, while TLR5M did not increase significantly after bacterial infection, which suggested TLR5S might play a more important role in antibacterial immunity. Then, the upregulation of some proinflammatory cytokines like IL1β, IL8, IL12 and TNF 2 further indicated spleen had initiated TLR induced inflammatory response to defense against invading organisms. However, NF-κB inhibitor alpha (NFKBIA) and inhibitor of NF-κB kinase (IKKE), which can inhibit the expression of proinflammatory cytokines, were also significantly upregulated in the spleens of zigzag eels. Similar expression patterns of TLR5, cytokines and NFKBIA have also been observed in blunt-snout bream infected with *A. hydrophila* [23] and rainbow brout challenged with *Yersinia ruckeri* O1 [44]. A previous study suggested that a strong inflammatory response could cause tissue damage [45]. Thus, the upregulation of NFKBIA and IKKE might contribute to decreasing inflammatory damage induced by pathogens. It is well known that TLR2 can recognize lipopeptides and that TLR7 can bind to single-stranded viral RNA. According to our qPCR analysis at three time points, TLR2 and TLR7 were first significantly downregulated at 12 h post infection and then recovered to normal level. Similarly, downregulation of TLR2 and TLR7 has also been reported in common carp [41] and large yellow croaker [45] after bacterial infection, which might indicate the expression of TLR2 and TLR7 was inhibited after bacterial infection. However, TLR7 was found to be significantly upregulated in large yellow croaker injected with poly (I:C) [45], which might indicate that TLRs have significantly different responses to specific and non-specific ligands. TLR14 belongs to the TLR2 subfamily, which can recognize various microorganism components such as bacterial peptidoglycan, lipoprotein, lipopolysaccharide in mammals [46]. However, little information is known about the precise recognition molecule of TLR14 in fish. Our qPCR analysis showed that TLR14 were significantly downregulated in Zigzag eel after bacterial infection, while in *Paralichthys olivaceus*, *Edwardsiella tarda* infection increased TLR14 gene expression from 1 to 6 day post infection [46]. These results suggested that TLR14 might play a different role in the immune response of Japanese flounder and Zigzag eel, which need to be further confirmed. Furthermore, the expression levels of TLR21, TLR22 and TLR23 in zigzag eel were also detected and only TLR22 did not change a lot after bacterial infection. Previous studies had demonstrated TLR21 was significantly upregulated by CpG-ODNs, poly (I:C), pathogenic bacteria and iridovirus [47], and TLR23 was also suggested to participate in bacterial and viral recognition [48]. It's interesting that TLR21 and TLR23 were significantly downregulated in zigzag eel after bacterial infection, which might indicate they respond to bacterial ligands in a different way. Fish TLR22 is usually deemed to participate in the anti-viral immunity [49,50]. Ahn et al. [48] and our study showed that TLR22 made no significant response to bacterial infection, suggesting TLR22 might not contribute to the anti-bacterial immunity.

Cytokines are soluble extracellular proteins or glycoproteins mainly including IL, TNF, colony stimulating factor (CSF), chemokines and growth factors such as transforming growth factor (TGF) [51]. Cytokines not only participate in immune regulation but also play an important role in the success of the reproductive process [51]. In this study, cytokine-related pathways such as cytokine-cytokine receptor interaction and TNF signaling pathway were all significantly enriched. In addition to upregulation of IL1β, IL8, IL12 and TNF2 in the TLR signaling pathway, many proinflammatory cytokines and corresponding receptors, such as IL6, IL17, TNF12, CCL4 (CC chemokine ligand 4), IL2Rβ, IL12Rβ, IL17RC, IL1R1, and IL1R2, were also significantly upregulated (Fig. S4), which demonstrated that a complicated inflammatory response occurred in the process of immune defense against bacterial infection in the spleens of zigzag eels. Among these cytokines and receptors, IL1β and IL8 have also been reported to be upregulated in miiuy croaker after infection with *Vibrio anguillarum* [37] and IL6, IL1R1, and IL1R2 of common carp upregulated in response to *Aeromonas hydrophila* infection [21]. In addition, the upregulation of vascular endothelial growth factors (VEGFs) in the spleens of zigzag eel can promote angiogenesis and increased capillary permeability during the inflammatory process [52]. However, IL22 and TGF-β were also upregulated, which could inhibit the inflammatory response and maintain the balance of immune system to avoid tissue damage [53,54]. *A. veronii* has been reported as an opportunistic pathogen participating in gastroenteritis and extraintestinal infections

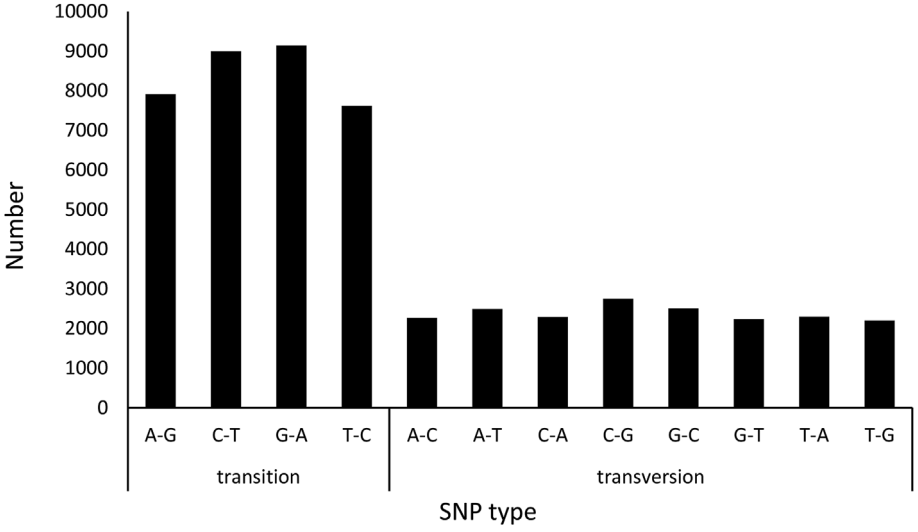

Fig. 9. Frequency distribution of SNPs based on different types.

[7]. The complex pathway of inflammatory bowel disease, characterized by chronic inflammation of the gastrointestinal tract, was also significantly enriched, indicating that ziazag eels could initiate a corresponding defensive response in the spleen after infection with *A. veronii*. A similar immune response involving TLRs and their downstream signaling pathways was also found in fish such as common carp and blunt snout bream [21,23]. Besides, there were also many differentially expressed genes participating in other immune related pathways like viral and parasitic diseases were also found to be significantly enriched, which indicated that zigzag eels had initiated a comprehensive immune response to resist bacterial invasion.

In conclusion, we performed a comparative analysis of zigzag eel spleens infected with *A. veronii* by using Illumina sequencing technology. A total of 110,328 unigenes were obtained, and 27,098 unigenes were successfully annotated by public protein databases, including Nr, UniProt, KEGG and KOG. In addition, 1278 unigenes were identified as differentially expressed genes. Moreover, GO and KEGG analysis revealed that many GO terms and pathways were involved in the host immune response mainly including toll-like receptor signaling pathway, cytokine-cytokine receptor interaction and TNF signaling pathway. In addition, according to transcriptome data and qPCR analysis, the expression levels of many TLRs and cytokines that participating in the inflammatory response changed a lot after *A. veronii* infection. These results provide us with much valuable information to better investigate the antibacterial immunity of zigzag eel.

Ethics statement

All the procedures and investigations were performed in accordance with the National Institutes of Health' Guide for the care and use of Laboratory animals (NIH Publications No. 8023, revised 1978).

Conflicts of interest

We declare that we have no financial or personal conflicts with other people or organizations.

Acknowledgements

This work was supported by the Youth Innovative Talents Program of Guangdong Provincial Department of Education [grant numbers 2016KQNCX118]; the Project of Science and Technology of Guangzhou city [grant numbers 201804010486, 201607020014]; the Science and Technology Project of Guangdong Province [grant numbers 2015B020235006, 2017B090904022], and the Basal Research Fund of the Central Public Interest Scientific Institution [grant numbers PM-zx021-201312-036, PM-zx703-201602-046].

Appendix A. Supplementary data

Supplementary data to this article can be found online at https://doi.org/10.1016/j.fsi.2019.02.020.

References

[1] R. Froese, D. Pauly (Eds.), FishBase. World Wide Web Electronic Publication, 2017 www.fishbase.org.
[2] H.M. Hossain MY, K. Yahya, Z.F. Ahmed, M.R.I. Sarder, M.A. Islam, K.K.U. Ahmed, Threatened fishes of the world: *Mastacembelus armatus* (Lacepede, 1800) (Synbranchiformes: Mastacembelidae), Croat. J. Fish. (73) (2015) 137–139.
[3] Q. Li, R. Xu, H. Shu, Q. Chen, J. Huang, The complete mitochondrial genome of the Zigzag eel *Mastacembelus armatus* (Teleostei, Mastacembelidae), Mitochondrial DNA Part A 27 (1) (2016) 330–331.
[4] J.M. Janda, S.L. Abbott, The genus *Aeromonas*: taxonomy, pathogenicity, and infection, Clin. Microbiol. Rev. 23 (1) (2010) 35–73.
[5] J.J. Havixbeck, A.M. Rieger, L.J. Churchill, D.R. Barreda, Neutrophils exert protection in early *Aeromonas veronii* infections through the clearance of both bacteria and dying macrophages, Fish Shellfish Immunol. 63 (2017) 18–30.
[6] P.K. Sahoo, K.D. Mahapatra, J.N. Saha, A. Barat, M. Sahoo, B.R. Mohanty, B. Gjerde, J. Odegard, M. Rye, R. Salte, Family association between immune parameters and resistance to *Aeromonas hydrophila* infection in the Indian major carp, *Labeo rohita*, Fish Shellfish Immunol. 25 (1–2) (2008) 163–169.
[7] R.C. Vazquez-Juarez, M. Gomez-Chiarri, H. Barrera-Saldana, N. Hernandez-Saavedra, S. Dumas, F. Ascencio, Evaluation of DNA vaccination of spotted sand bass (*Paralabrax maculatofasciatus*) with two major outer-membrane protein-encoding genes from *Aeromonas veronii*, Fish Shellfish Immunol. 19 (2) (2005) 153–163.
[8] D.X. Zhang, Y.H. Kang, L. Chen, S.A. Siddiqui, C.F. Wang, A.D. Qian, X.F. Shan, Oral immunization with recombinant Lactobacillus casei expressing OmpAI confers protection against *Aeromonas veronii* challenge in common carp, *Cyprinus carpio*, Fish Shellfish Immunol. 72 (2018) 552–563.
[9] N. Abu-Elala, M. Abdelsalam, S. Marouf, A. Setta, Comparative analysis of virulence genes, antibiotic resistance and gyrB-based phylogeny of motile *Aeromonas* species isolates from Nile tilapia and domestic fowl, Lett. Appl. Microbiol. 61 (5) (2015) 429–436.
[10] A.P. Zepeda-Velazquez, V. Vega-Sanchez, C. Ortega-Santana, M. Rubio-Godoy, D.M. de Oca-Mira, E. Soriano-Vargas, Pathogenicity of Mexican isolates of *Aeromonas* sp. in immersion experimentally-infected rainbow trout (*Oncorhynchus mykiss*, Walbaum 1792), Acta Trop. 169 (2017) 122–124.
[11] D. Zhang, L. Liu, N. Li, Y. Ren, Q. Lin, C. Shi, S. Wu, Epidemic characteristics of different species of *Aeromonas* in diseased fish in southern China, Fish. Sci. 34 (11) (2015) 673–682.
[12] N. Narejo, S. Rahmatullah, M. Rashid, Studies on the reproductive biology of freshwater spiny eel, *Mastacembalus armatus* (Lacepede) reared in the cemented cisterns of BAU, Mymensingh, Bangladesh, Pakist, J. Biol. Sci. 5 (7) (2002) 809–811.
[13] M. Rahman, G. Ahmed, S. Rahmatullah, Fecundity of wild freshwater spiny eel *Mastacembelus armatus* Lacepede from Mymensingh region of Bangladesh, Asian Fish Sci. 19 (2006) 51–59.
[14] M. Ali, M. Rahman, M. Sarder, M. Mollah, Histological study of the developing gonads of endangered freshwater spiny eel, *Mastacembelus armatus* during the reproductive cycle, J. Bangladesh Agric. Univ. 14 (2) (2016) 261–269.
[15] A. Vankara, V. Chikkam, Histopathology of heart of freshwater spiny eel, *Mastacembelus armatus* naturally infected with *Tetracotyle metacercaria* (trematoda: Strigeidae), Res. J. Parasitol. 8 (2) (2013) 45–54.
[16] A.P. Vankara, G. Mani, C. Vijayalaks, Metazoan parasite infracommunities of the freshwater eel, *Mastacembelus armatus* Lacèpéde, 1800 from river Godavari, India, Int. J. Zool. Res. 7 (1) (2011) 19–33.
[17] S. Nanware, D. Bhure, Intestinal histopathology of *Mastacembelus armatus* 13 parasitized by *pseudophyllidean cestodes*, Flora 22 (1) (2016) 125–130.
[18] H. Yang, Q. Li, H. Shu, L. Yue, T. Lin, Y. Liu, Genetic diversity of *Mastacembelus armatus* in southern China and surrounding areas based on ISSR analysis, Acta Hydrobiol. Sin. 40 (2016) 63–70.
[19] V. Uthayakumar, V. Ramasubramanian, D. Senthilkumar, V.B. Priyadarisini, R. Harikrishnan, Biochemical characterization, antimicrobial and hemolytic studies on skin mucus of fresh water spiny eel *Mastacembelus armatus*, Asian Pac. J. Trop. Biomed. 2 (2) (2012) S863–S869.
[20] C. Han, Q. Li, Z. Zhang, J. Huang, Characterization, expression, and evolutionary analysis of new TLR3 and TLR5M genes cloned from the spiny eel *Mastacembelus armatus*, Dev. Comp. Immunol. 77 (2017) 174–187.
[21] Y. Jiang, S. Feng, S. Zhang, H. Liu, J. Feng, X. Mu, X. Sun, P. Xu, Transcriptome signatures in common carp spleen in response to *Aeromonas hydrophila* infection, Fish Shellfish Immunol. 57 (2016) 41–48.
[22] R. Kumar, P. Sahoo, B. A, Transcriptome profiling and expression analysis of immune responsive genes in the liver of Golden mahseer (*Tor putitora*) challenged with *Aeromonas hydrophila*, Fish Shellfish Immunol. (67) (2017) 655–666.
[23] N. Tran, Z. Gao, H. Zhao, S. Yi, B. Chen, Y. Zhao, L. Lin, X. Liu, W. Wang, Transcriptome analysis and microsatellite discovery in the blunt snout bream (*Megalobrama amblycephala*) after challenge with *Aeromonas hydrophila*, Fish Shellfish Immunol. 45 (1) (2015) 72–82.
[24] M.G. Grabherr, B.J. Haas, M. Yassour, J.Z. Levin, D.A. Thompson, I. Amit, X. Adiconis, L. Fan, R. Raychowdhury, Q. Zeng, Z. Chen, E. Mauceli, N. Hacohen, A. Gnirke, N. Rhind, F. di Palma, B.W. Birren, C. Nusbaum, K. Lindblad-Toh, N. Friedman, A. Regev, Full-length transcriptome assembly from RNA-Seq data without a reference genome, Nat. Biotechnol. 29 (7) (2011) 644–652.
[25] A. Conesa, S. Götz, J. García-Gómez, J. Terol, M. Talón, M. Robles, Blast2GO: a universal tool for annotation, visualization and analysis in functional genomics research, Bioinformatics 21 (2005) 3674–3676.
[26] J. Ye, L. Fang, H. Zheng, Y. Zhang, J. Chen, Z. Zhang, J. Wang, S. Li, R. Li, L. Bolund, J. Wang, WEGO: a web tool for plotting GO annotations, Nucleic Acids Res. 34 (2006) W293–W297.
[27] M. Kanehisa, S. Goto, S. Kawashima, Y. Okuno, M. Hattori, The KEGG resource for deciphering the genome, Nucleic Acids Res. 32 (2004) D277–D280.
[28] B. Langmead, S.L. Salzberg, Fast gapped-read alignment with Bowtie 2, Nat. Methods 9 (4) (2012) 357–359.
[29] K.J. Livak, T.D. Schmittgen, Analysis of relative gene expression data using real-time quantitative PCR and the 2(-Delta Delta C (T)) Method, Methods 25 (4) (2001) 402–408.
[30] T. Thiel, W. Michalek, R.K. Varshney, A. Graner, Exploiting EST databases for the development and characterization of gene-derived SSR-markers in barley (*Hordeum vulgare* L.), Theor. Appl. Genet. 106 (3) (2003) 411–422.
[31] A. Untergasser, I. Cutcutache, T. Koressaar, J. Ye, B.C. Faircloth, M. Remm, S.G. Rozen, Primer3–new capabilities and interfaces, Nucleic Acids Res. 40 (15) (2012) e115.
[32] R. Li, Y. Li, K. Kristiansen, J. Wang, SOAP: short oligonucleotide alignment

program, Bioinformatics 24 (5) (2008) 713–714.
[33] C. Li, Y. Zhang, R. Wang, J. Lu, S. Nandi, S. Mohanty, J. Terhune, Z. Liu, E. Peatman, RNA-seq analysis of mucosal immune responses reveals signatures of intestinal barrier disruption and pathogen entry following *Edwardsiella ictaluri* infection in channel catfish, *Ictalurus punctatus*, Fish Shellfish Immunol. 32 (5) (2012) 816–827.
[34] J. Ge, S. Chen, C. Liu, L. Bian, H. Sun, J. Tan, Characterization of the global transcriptome and microsatellite marker information for spotted halibut *Verasper variegatus*, Genes Genomes 39 (3) (2016) 307–316.
[35] J. Wang, B. Lindsay, J. Leebens-Mack, L. Cui, K. Wall, W. Miller, C. de Pamphilis, EST clustering error evaluation and correction, Bioinformatics 20 (2004) 2973–2984.
[36] T. Liu, S. Zhu, Q. Tang, P. Chen, Y. Yu, S. Tang, De novo assembly and characterization of transcriptome using Illumina paired-end sequencing and identification of CesA gene in ramie (*Boehmeria nivea* L. Gaud), BMC Genomics 14 (2013) 125.
[37] R. Che, Y. Sun, D. Sun, T. Xu, Characterization of the miiuy croaker (*Miichthys miiuy*) transcriptome and development of immune-relevant genes and molecular markers, PLoS One 9 (4) (2014) e94046.
[38] C. Qin, Q. Gong, Z. Wen, D. Yuan, T. Shao, J. Wang, H. Li, Transcriptome analysis of the spleen of the darkbarbel catfish *Pelteobagrus vachellii* in response to *Aeromonas hydrophila* infection, Fish Shellfish Immunol. (70) (2017) 498–506.
[39] S. Akira, K. Takeda, Toll-like receptor signalling, Nat. Rev. Immunol. 4 (7) (2004) 499–511.
[40] S. Akira, S. Uematsu, O. Takeuchi, Pathogen recognition and innate immunity, Cell 124 (2006) 783–801.
[41] Y. Gong, S. Feng, S. Li, Y. Zhang, Z. Zhao, M. Hu, P. Xu, Y. Jiang, Genome-wide characterization of Toll-like receptor gene family in common carp (*Cyprinus carpio*) and their involvement in host immune response to *Aeromonas hydrophila* infection, Comp. Biochem. Physiol. Part D 24 (2017) 89–98.
[42] R. Lai, I. Jakovlić, H. Liu, F. Zhan, J. Wei, W. Wang, Molecular characterization and immunological response analysis of toll-like receptors from the blunt snout bream (*Megalobrama amblycephala*), Dev. Comp. Immunol. 67 (2016) 471–475.
[43] A. Didierlaurent, I. Ferrero, L.A. Otten, B. Dubois, M. Reinhardt, H. Carlsen, R. Blomhoff, S. Akira, J.P. Kraehenbuhl, J.C. Sirard, Flagellin promotes myeloid differentiation factor 88-dependent development of Th2-type response, J. Immunol. 172 (11) (2004) 6922–6930.
[44] M.K. Raida, K. Buchmann, Innate immune response in rainbow trout (*Oncorhynchus mykiss*) against primary and secondary infections with *Yersinia ruckeri* O1, Dev. Comp. Immunol. 33 (1) (2009) 35–45.
[45] T. Qian, K. Wang, Y. Mu, J. Ao, X. Chen, Molecular characterization and expression analysis of TLR 7 and TLR 8 homologs in large yellow croaker (*Pseudosciaena crocea*), Fish Shellfish Immunol. 35 (3) (2013) 671–679.
[46] S.D. Hwang, H. Kondo, I. Hirono, T. Aoki, Molecular cloning and characterization of toll-like receptor 14 in Japanese flounder, *Paralichthys olivaceus*, Fish Shellfish Immunol. 30 (1) (2011) 425–429.
[47] M. Sun, Y. Mu, Y. Ding, J. Ao, X. Chen, Molecular and functional characterization of toll-like receptor 21 in large yellow croaker (*larimichthys crocea*), Fish Shellfish Immunol. 59 (2016) 179–188.
[48] d. H. Ahn, S.C. Shin, H. Park, Characterization of toll-like receptor gene expression and the pathogen agonist response in the antarctic bullhead notothen *Notothenia coriiceps*, Immunogenetics 66 (9–10) (2014) 563–573.
[49] A. Matsuo, H. Oshiumi, T. Tsujita, H. Mitani, H. Kasai, M. Yoshimizu, et al., Teleost TLR22 recognizes RNA duplex to induce IFN and protect cells from birnaviruses, J. Immunol. 181 (2008) 3474–3485.
[50] X. Ding, Y. Liang, W. Peng, R. Li, H. Lin, Y. Zhang, et al., Intracellular TLR22 acts as an inflammation equalizer via suppression of NF-κB and selective activation of MAPK pathway in fish, Fish Shellfish Immunol. 72 (2018) 646–657.
[51] W. Ingman, R. Jones, Cytokine knockouts in reproduction: the use of gene ablation to dissect roles of cytokines in reproductive biology, Hum. Reprod. Update 14 (2) (2008) 179–192.
[52] N. Ferrara, T. Davissmyth, The biology of vascular endothelial growth factor, Endocr. Rev. 18 (1) (2013) 4–25.
[53] L.A. Zenewicz, G.D. Yancopoulos, D.M. Valenzuela, A.J. Murphy, S. Stevens, R.A. Flavell, Innate and adaptive interleukin-22 protects mice from inflammatory bowel disease, Immunity 29 (6) (2008) 947–957.
[54] J. Massagué, TGF-β Signal transduction, Annu. Rev. Biochem. 67 (67) (2003) 753–791.